



## Freeze-drying process for the design of porous formulations based on bismuth-potassium-ammonium citrate

Ekaterina S. Naydenko, Tatyana Yu. Podlipskaya, Yurii M. Yukhin & Andrey G. Ogienko

To cite this article: Ekaterina S. Naydenko, Tatyana Yu. Podlipskaya, Yurii M. Yukhin & Andrey G. Ogienko (2020): Freeze-drying process for the design of porous formulations based on bismuth-potassium-ammonium citrate, Journal of Dispersion Science and Technology, DOI: [10.1080/01932691.2020.1711770](https://doi.org/10.1080/01932691.2020.1711770)

To link to this article: <https://doi.org/10.1080/01932691.2020.1711770>

 View supplementary material [↗](#)

 Published online: 16 Jan 2020.

 Submit your article to this journal [↗](#)

 Article views: 10

 View related articles [↗](#)

 View Crossmark data [↗](#)

# Freeze-drying process for the design of porous formulations based on bismuth-potassium-ammonium citrate

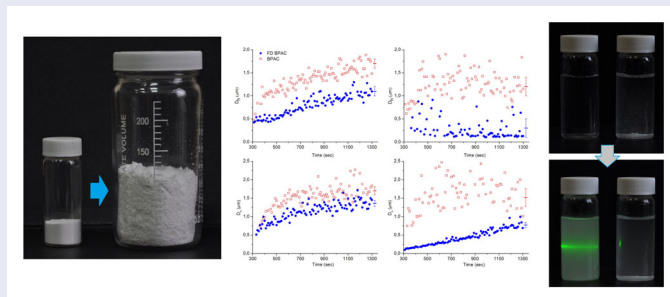
Ekaterina S. Naydenko<sup>a</sup>, Tatyana Yu. Podlipskaya<sup>b</sup>, Yurii M. Yukhin<sup>a</sup>, and Andrey G. Ogienko<sup>b,c</sup> 

<sup>a</sup>Institute of Solid State Chemistry and Mechanochemistry, Siberian Branch of the Russian Academy of Sciences, Novosibirsk, Russia; <sup>b</sup>Nikolaev Institute of Inorganic Chemistry, Siberian Branch of the Russian Academy of Sciences, Novosibirsk, Russia; <sup>c</sup>Department of Natural Sciences, Novosibirsk State University, Novosibirsk, Russia

## ABSTRACT

The objective of this study was to find optimal freeze-drying process parameters to design porous and friable freeze-dried bismuth-potassium-ammonium citrate (FD BPAC) with improved dissolution behavior. The nucleation and melting temperatures of frozen BPAC solution in water and tert-butanol/water co-solvent system were studied with use of thermal analysis. The phases that resulted on cooling were studied by low-temperature powder x-ray diffraction. BPAC formed an amorphous freeze concentrate on cooling and remained amorphous during freeze-drying and subsequent storage. The nucleation of colloidal bismuth subcitrate (CBS) in the FD BPAC and starting BPAC systems in 0.1 M and 0.01 M HCl was studied by dynamic light scattering (DLS) method. The proposed preparation method of FD BPAC can be the basis for design of formulations with enhanced dissolution rate for bismuth-based triple/quadruple therapy, where FD BPAC simultaneously act as a carrier and an active ingredient.

## GRAPHICAL ABSTRACT



## ARTICLE HISTORY

Received 11 October 2018  
Accepted 31 August 2019

## KEYWORDS

Bismuth-potassium-ammonium citrate; freeze-drying; dynamic light scattering; nucleation

## 1. Introduction

Colloidal bismuth subcitrate (CBS) has been widely used for the treatment of gastrointestinal disorders and *Helicobacter pylori* (*H. pylori*) infection.<sup>[1–4]</sup> CBS is an active ingredient of anti-ulcer formulations for bismuth-based triple/quadruple therapy<sup>[5–8]</sup> such as BMT (sold under license as Pylera®, consisting of potassium bismuth subcitrate, metronidazole and tetracycline).<sup>[8]</sup> CBS forms a protective film on the ulcer surface in the acidic stomach environment, hindering the action of hydrochloric acid and pepsin<sup>[3]</sup> and also enhances the mucus formation, stimulates bicarbonates secretion and the synthesis of prostaglandins in the stomach wall.<sup>[9]</sup> The most common CBS preparation methods described in different publications and patents are crystallization,<sup>[10]</sup> antisolvent precipitation by acetone from an aqueous solution of

potassium citrate, bismuth citrate and potassium hydroxide<sup>[11]</sup> and spray drying of an aqueous ammonia solution of colloidal bismuth citrate.<sup>[12]</sup>

Freeze-drying (lyophilization) is a drying technology widely used in the pharmaceutical industry.<sup>[13]</sup> It provides products with desired physicochemical properties, such as enhanced dissolution rates and bioavailability.<sup>[14–17]</sup> Among several organic-water co-solvent systems, “tert-butanol (TBA) – water” is of particular interest because of its low toxicity, low residual content, high eutectic melting temperatures, low sublimation enthalpy and high vapor pressure.<sup>[18–20]</sup> Moreover, many studies show that the addition of TBA can considerably enhance the sublimation rate, resulting in shortening of the drying cycles.<sup>[18–23]</sup> Therefore, for economy concerns it is desirable to apply freeze-drying

**CONTACT** Andrey G. Ogienko  andreyogienko@gmail.com  Nikolaev Institute of Inorganic Chemistry, Siberian Branch of the Russian Academy of Sciences, Novosibirsk 630090, Russia.

Color versions of one or more of the figures in the article can be found online at [www.tandfonline.com/ldis](http://www.tandfonline.com/ldis).

 Supplemental data for this article is available online at <https://doi.org/10.1080/01932691.2020.1711770>.

to bismuth-potassium-ammonium citrate using TBA/water co-solvent system.

The aim of this study was to find optimal freeze-drying process parameters by combination of thermal analysis and low-temperature powder x-ray diffraction experiments for producing porous and friable bismuth-potassium-ammonium citrate lyophiles (hereafter “FD BPAC”) with enhanced dissolution behavior and to study the nucleation of colloidal bismuth subcitrate in the FD BPAC and starting BPAC systems in 0.1 M and 0.01 M HCl. To the best of our knowledge, this is the first report of the FD BPAC preparation method and it can be the basis for design of formulations with enhanced dissolution rate for bismuth-based triple therapy, where FD BPAC simultaneously acts as a carrier and an active ingredient.

## 2. Experimental section

### 2.1. Material

Twice-distilled *tert*-butanol and distilled water were used as solvents. All chemicals were at least of analytical grade and were used as purchased without additional purification.

### 2.2. Samples for TA and low-temperature powder x-ray diffraction experiments

Starting solutions for powder x-ray diffraction and TA experiments were: pure water and TBA-water solution (10 wt % of TBA) (reference solutions for TA); aqueous BPAC solution (10 wt %); BPAC (7 wt %) solution in the TBA/water co-solvent system (10 wt % of TBA).

### 2.3. Low-temperature powder x-ray diffraction

Powder x-ray diffraction experiments were carried out on a Bruker D8 Advance diffractometer ( $\lambda = 1.5406 \text{ \AA}$ , tube voltage of 40 kV and tube current of 40 mA) equipped with an Anton Paar TTK 450 low temperature chamber. Vials (Sci/Spec, B69308) were filled with 1 ml of BPAC solutions, tightly closed with a PTFE cap and placed into an air thermostat at  $-20^\circ\text{C}$  (freezing time ca. 1 hour). The vial with frozen solution was broken, the sample was carefully but gently ground in a mortar (all operations were performed at liquid nitrogen temperature) and placed onto a holder, which had been preliminary cooled down to  $-120^\circ\text{C}$ . Diffraction patterns were measured in the  $-100$  –  $-5^\circ\text{C}$  temperature range ( $2\Theta$  scans in the 5–45 degree range, 0.02 degrees step).

### 2.4. TA experiments

The thermal analysis (TA) experiments, aimed to study the nucleation and melting temperatures in binary (TBA-water; BPAC-water) and ternary (BPAC-TBA-water) systems were carried out on the TA installation.<sup>[24]</sup> The signals registered using precision converter of signals of resistance thermometers and thermocouples “TERCON” with the switch of input

signals “TERCON-K” (TERMEX, Tomsk, Russia). An aluminum sample holder was loaded with four Teflon cells charged with solutions (the volume of the samples was 1.00 ml; the thickness of the solution layer in each of the cells was 13 mm). Type K thermocouple was placed in each of the samples, the junction being approximately in the middle of the sample. The assembly of the samples was placed in the autoclave. Then the autoclave was cooled/heated ( $+20^\circ\text{C} \rightarrow -40^\circ\text{C} \rightarrow +20^\circ\text{C}$ ) at the constant rate of  $0.5^\circ\text{C}/\text{min}$  at atmospheric pressure. The temperatures in each of the samples were digitally recorded. The absolute temperature uncertainty was  $\pm 0.2^\circ\text{C}$ . The formation of ice *Ih* and the “ice *Ih*-TBA·2H<sub>2</sub>O” eutectic on freezing (nucleation) as well as melting of ice *Ih*, the “ice *Ih*-TBA·2H<sub>2</sub>O” eutectic in binary and ternary systems on heating were revealed by heat effects registered with the thermocouple. All measurements were performed three times. Typical experimental curves are shown in the ESI (Supplementary material Figure S1 in the ESI).

### 2.5. Preparation of BPAC

A bismuth solution with 400 g/L of bismuth was prepared by dissolving bismuth oxide in 6 M HNO<sub>3</sub>. BPAC was prepared according to [10] in several steps: i) bismuth precipitation in the form of oxohydroxonitrate with the composition  $[\text{Bi}_6\text{O}_4(\text{OH})_4](\text{NO}_3)_6 \cdot \text{H}_2\text{O}$  at pH 0.5–1.2 and the temperature of  $50$ – $70^\circ\text{C}$  [31]; ii) its conversion into citrate with the composition  $\text{BiC}_6\text{H}_5\text{O}_7$  by treatment with a solution of citric acid; iii) dissolution of bismuth citrate in an aqueous solution of potassium hydroxide in the presence of ammonium hydroxide; iv) crystallization BPAC by evaporation at  $65 \pm 5^\circ\text{C}$ .

### 2.6. Preparation of FD BPAC

Freeze-drying was accomplished with laboratory-scale freeze dryer (1 processing shelf, 25.0 cm × 35.0 cm (temperature range of  $35 \div +80^\circ\text{C}$ )) (NIIC SB RAS, Russia) equipped with an organic solvent trap. Starting BPAC solution (7 wt. %) in the TBA/water co-solvent system (10 wt. % of TBA) was prepared by weight. The drying tray was filled with 35 g of BPAC solution (filling depth 7 mm) and placed overnight (ca. 12 hours) onto the shelf preliminary cooled to  $-20^\circ\text{C}$ . Freeze-drying was carried out at shelf temperature of  $-20^\circ\text{C}$  until the pressure dropped to  $P < 17 \text{ mTorr}$ ; then the shelf temperature was increased to  $+30^\circ\text{C}$  and this temperature was kept for 4 hours. After that the pressure in the freeze dryer was increased up to  $P = 1 \text{ bar}$  by filling it with dry nitrogen.

### 2.7. Determination of Bi(III) content in BPAC and FD BPAC

Bi(III) was determined by titration with 0.01 M EDTA, using xylenol orange as the indicator, the maximum error in bismuth content determination being 2.0%.

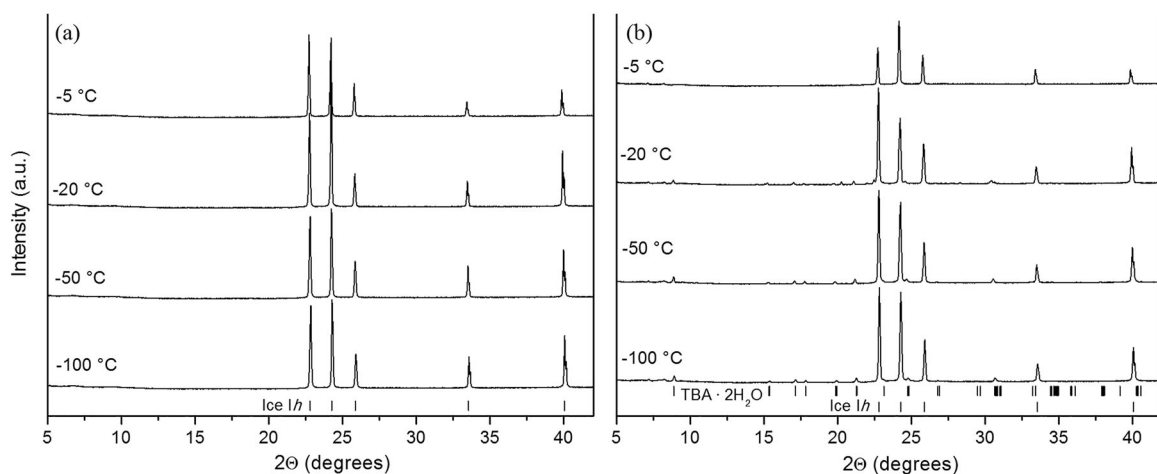


**Figure 1.** Powder XRD patterns of the frozen aqueous BPAC solution (10 wt % of BPAC) and BPAC solution (7 wt % of BPAC) in TBA/water co-solvent system (10 wt % of TBA) at different temperatures. The positions of the reflections of the TBA·2H<sub>2</sub>O and ice Ih are shown as ticks at the bottom.

## 2.8. SEM experiments

Morphological examination of the FD BPAC and BPAC samples was carried out with TM-1000 (Hitachi) scanning electron microscope. The samples were mounted on a SEM stub with double-sided carbon tape and coated with gold (thickness about 8 nm) with a JFC-1600 Auto Fine Coater (Jeol).

## 2.9. Infrared spectroscopy experiments

The IR absorption spectra of the FD BPAC and BPAC samples were recorded in KBr tablets at room temperature (the volume ratio KBr: sample = 200: 1) on a Scimitar FTS 2000 (Digilab, USA) spectrometer within wavenumber range 400 cm<sup>-1</sup> to 4000 cm<sup>-1</sup> with resolution of 4 cm<sup>-1</sup>.

## 2.10. Dynamic light scattering experiments

Nucleation of bismuth colloidal subcitrate in the FD BPAC and BPAC systems in 0.1 M and 0.01 M HCl were analyzed by DLS method. The weighed samples (50/40/30/20 mg) were placed at the bottom of vials (Sci/Spec, B75592) and filled with 20 ml of 0.1 M or 0.01 M HCl at ambient temperature (+20 °C), then the closed vials were vigorously shaken (5 seconds). The effective hydrodynamic diameters ( $D_h$ ) of particles were determined by NanoBrook Omni spectrometer (Brookhaven, USA) with use of method of cumulants by monomodal analysis. The power of the solid-state laser was 35 mW, the wavelength 640 nm; the scattered photons were accumulated using a high-sensitive APDx detector at a 90° angle to the radiation source. Photon accumulation time was 10 seconds (due to rapid sedimentation), and the number of photons for building the autocorrelation function was 10<sup>5</sup>–10<sup>6</sup>. The measurements were carried out in 1-cm polystyrene cells at 20 °C; the temperature was maintained with the accuracy of 0.1 °C. The Z-averaged (by intensity) hydrodynamic diameters were calculated by the Stokes–Einstein equation for spherical particles.<sup>[25]</sup>

## 2.11. The visual observation of the dissolution behavior and nucleation of bismuth colloidal subcitrate of the FD BPAC and BPAC in 0.1 M and 0.01 M HCl

The dissolution behavior and nucleation of bismuth colloidal subcitrate of the FD BPAC in 0.1 M and 0.01 M HCl were compared with that of BPAC used as a reference. The weighed samples were placed at the bottom of vials (Sci/Spec, B75592) and filled with 0.1/0.01 M HCl at ambient temperature (+20 °C), then the closed vials were vigorously shaken (5 seconds). The changes occurring with the solutions were recorded with a digital photo camera at regular time intervals. Photo- and video data are presented as [Supplementary material Figures S4-S5](#) and [vial.mpg](#) in the Supporting Information.

## 3. Results and discussion

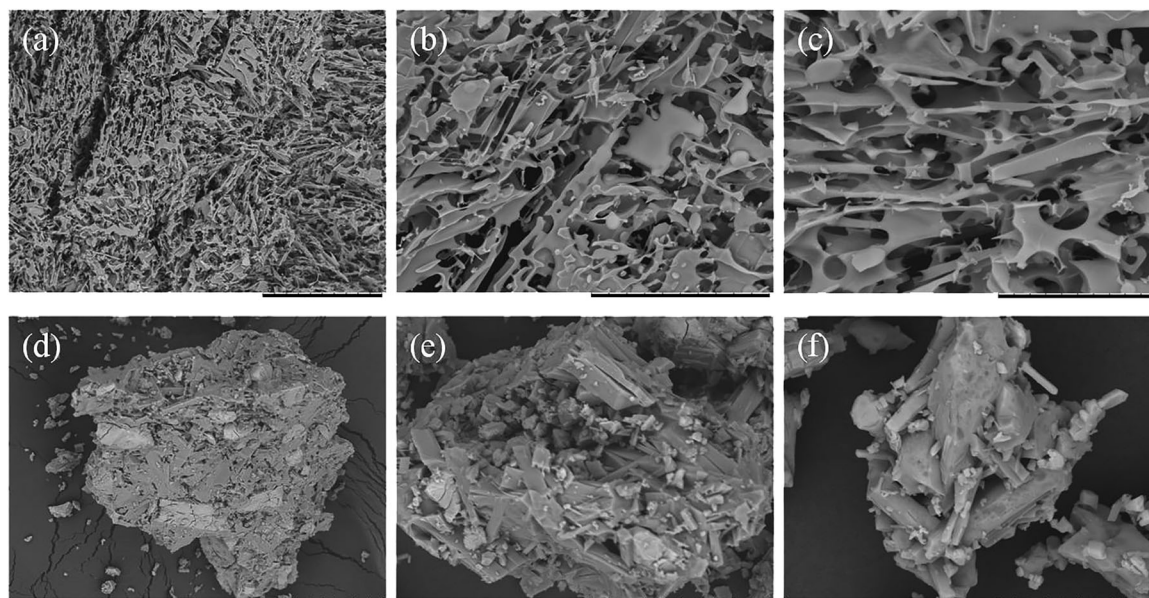
### 3.1. Formulation parameters and freezing/primary drying temperature determination

Low-temperature powder x-ray diffraction experiments (details are given in ESI), carried out with samples of frozen BPAC aqueous solution and BPAC solution in the TBA/water co-solvent system ([Figure 1](#)), revealed that BPAC formed an amorphous freeze concentrate under conditions (freezing at –20 °C) provided by typical laboratory freeze-dryers. For the aqueous solution, ice Ih is the only crystalline phase in the whole temperature range studied; for the TBA/water co-solvent system the diffraction patterns, in addition to ice Ih reflections, exhibit reflections of the TBA·2H<sub>2</sub>O hydrate; the increase in temperature (from –100 to –5 °C) did not result in the appearance of any reflections corresponding to BPAC or any other crystalline phases. On the diffraction patterns recorded at –5 °C only reflections corresponding to ice Ih were present (ice Ih coexists with the aqueous solution of BPAC and with BPAC solution in TBA/water).

Results of TA experiments (details are given in ESI), aimed to identify the nucleation and eutectic melting temperatures in binary (BPAC-water) and ternary (BPAC-TBA-water) systems are listed in [Table 1](#). No thermal effects corresponding to crystallization and melting of the binary

**Table 1.** Results of TA experiments, aimed to identify the nucleation and eutectic melting temperatures in binary (TBA-water; water-BPAC) and ternary (TBA-water-BPAC) systems.

| Formulation    | Nucleation temperature $\pm$ e.s.d., °C/(interval), °C | Phase nucleated (N)/crystallized (C)                                      | Melting temperature $\pm$ e.s.d., °C  | Phase melted  |
|----------------|--|---|---|---|
| Water          | $-6.5 \pm 0.5$<br>( $-5.2 \div -7.0$ )                 | ice <i>Ih</i> (N)   | $-0.1 \pm 0.1$  | ice <i>Ih</i>   |
| BPAC-water     | $-7.0 \pm 0.5$<br>( $-6.5 \div -7.9$ )                 | ice <i>Ih</i> (N)   | $-2.9 \pm 0.1$  | ice <i>Ih</i>   |
| BPAC-TBA-water | $-15.4 \pm 0.2$<br>( $-15.1 \div -15.6$ )              | “ice <i>Ih</i> -TBA·2H <sub>2</sub> O” eutectic in the ternary system (C) | $-10.9 \pm 0.2$<br>( $-9.5 \div -10.5$ metastable “ice <i>Ih</i> -TBA·2H <sub>2</sub> O” eutectic in TBA-water system) <sup>[26–28]</sup> | “ice <i>Ih</i> -TBA·2H <sub>2</sub> O” eutectic in the presence of amorphous BPAC |

**Figure 2.** SEM images of the FD BPAC (a, b, c) and starting BPAC (d, e, f). Scale bar: a, d: 100  $\mu$ m; b, e: 50  $\mu$ m; c, f: 20  $\mu$ m.

eutectic “BPAC-water” in the ternary system “BPAC-TBA-water” were observed, also in agreement with the powder x-ray diffraction data on amorphization of BPAC on freezing of the BPAC solution in the TBA/water co-solvent system. Two thermal effects at  $-10.9 \pm 0.2^\circ\text{C}$  and  $-3.2^\circ\text{C}$  (“diffuse”) were observed on TA curves on warming of the frozen sample of BPAC solution in the TBA/water co-solvent system. The thermal effect at  $-10.9 \pm 0.2^\circ\text{C}$  was assigned to melting of the “ice *Ih* - TBA·2H<sub>2</sub>O” eutectic ( $-9.5 \div -10.5$  metastable eutectic “ice *Ih* - TBA·2H<sub>2</sub>O” in TBA-water system)<sup>[26–28]</sup> in the presence of amorphous BPAC [in the case of formation of the crystalline phase of the dissolved salt – to the melting of the “TBA·2H<sub>2</sub>O – BPAC - ice *Ih*” ternary eutectic], and the thermal effect at  $-3.2^\circ\text{C}$  – to ice *Ih* melting (liquidus curve) in the “BPAC-TBA-water” quaternary system. The ternary eutectic melting temperature in the “BPAC-TBA-water” system ( $-10.9^\circ\text{C}$ ) is the critical temperature of the primary drying. In order to achieve complete solidification of the starting solution, it is necessary to provide freezing temperature below  $-15.6^\circ\text{C}$ .

### 3.2. Characterization

The freeze dried BPAC (hereafter “FD BPAC”) was light fluffy powder demonstrating low bulk density (Supplementary

material Figure S2a ESI). Visual inspection of the obtained sample revealed a conventional freeze-dried cake lacking any signs of skin on the cake surface and collapsed inclusions near the bottom of the drying trays (Supplementary material Figure S2b ESI). According to SEM data (Figure 2), the FD BPAC cake surface was characterized by elongated fissures (50–100  $\mu$ m), and internal cake morphology is similar in its appearance. Cases of partial collapse in the lamellar structure, as would be indicated by small droplets, have not been observed. XRD experiments revealed that BPAC undergoes amorphization on cooling and remain amorphous during freeze-drying (Supplementary material Figure S3 ESI). BPAC and FD BPAC identity was confirmed by IR spectroscopic data (Supplementary material Figure S4 ESI). Analytical results for bismuth content in BPAC and FD BPAC are 33.66 and 33.42 wt %, respectively (*calcd.* 32.7–38.2 wt %).

Experiments on dissolution behavior of the FD BPAC and BPAC and nucleation of CBS were carried out with use of aqueous HCl solutions (pH = 1; pH = 2) as dissolution media, which more close to the basal pH values in patients with gastritis, gastric ulcer, duodenal ulcer as well as in normal subjects.<sup>[29]</sup> Preliminary experiments has shown that FD BPAC immediately dissolve in 0.1M/0.01M HCl and forms a homogeneous solution in contrast to the starting BPAC which does not dissolve completely (even in the case of

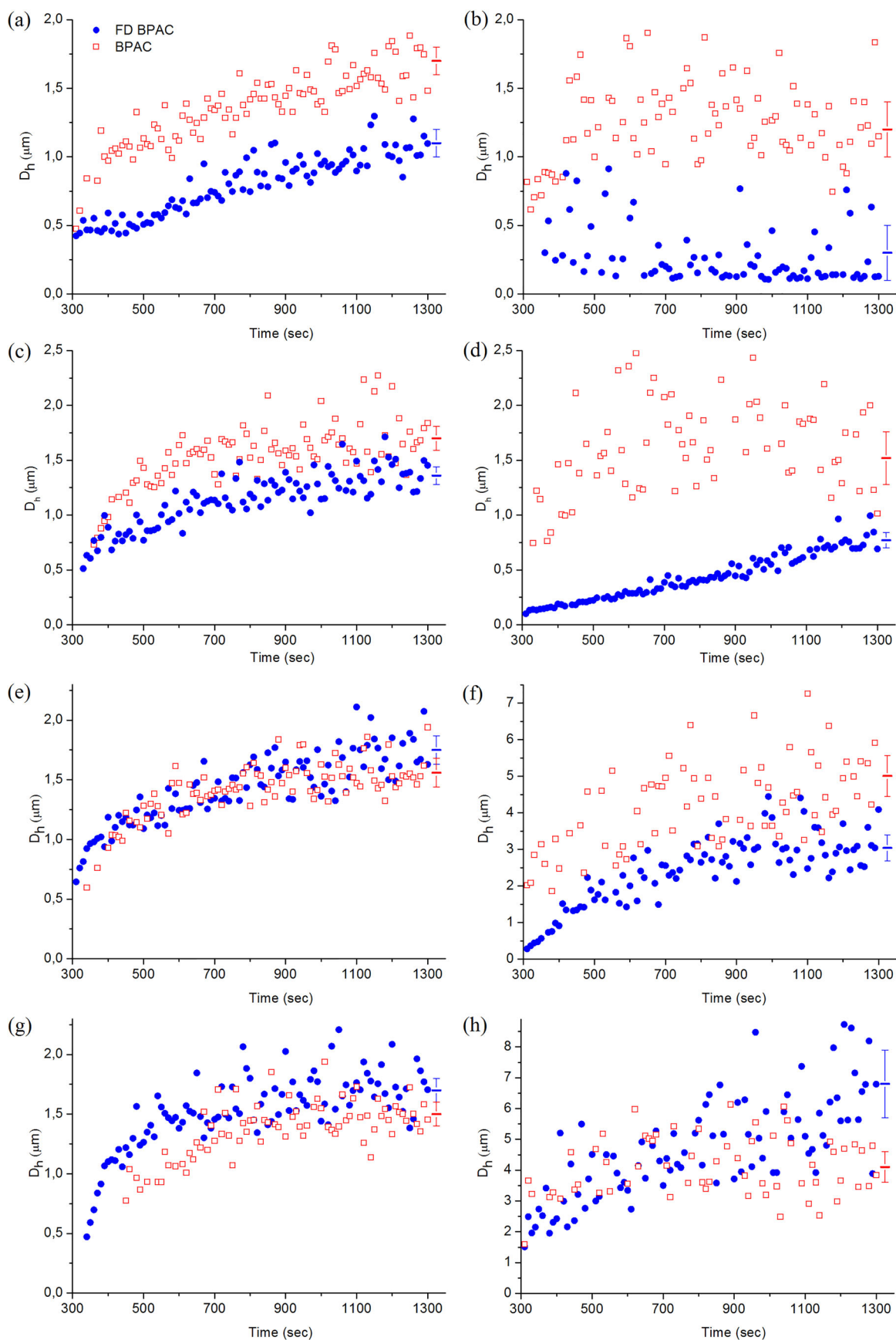


**Figure 3.** Time dependence of the effective hydrodynamic diameter ( $D_h$ ) of the bismuth colloidal subcitrate in the FD BPAC and BPAC systems (a, b: 50 mg; c, d: 40 mg; e, f: 30 mg; g, h: 20 mg) in 20 ml of 0.1 M (a, c, e, g) and 0.01 M (b, d, f, h) HCl. The starting solutions/suspensions were not filtered. Average values of hydrodynamic diameter, calculated from the last 10 values (error bars are given for the probability level of 95%) are shown on the right side of each data set.

**Table 2.** Results of DLS experiments, aimed to determine the effective hydrodynamic diameter ( $D_h$ ) of the bismuth colloidal subcitrate in the FD BPAC and BPAC mixtures in 0.1 M and 0.01 M HCl (20 minutes after mixing).

| $C_{HCl}$ , M | Sample mass in 20 ml of HCl | $D_h$ , $\mu\text{m}$ |           |
|---------------|-----------------------------|-----------------------|-----------|
|               |                             | FD BPAC               | BPAC      |
| 0.1           | 50 mg                       | 1.1 ± 0.1             | 1.7 ± 0.1 |
|               | 40 mg                       | 1.4 ± 0.1             | 1.7 ± 0.1 |
|               | 30 mg                       | 1.8 ± 0.1             | 1.6 ± 0.1 |
|               | 20 mg                       | 1.7 ± 0.1             | 1.5 ± 0.1 |
| 0.01          | 50 mg                       | 0.3 ± 0.2             | 1.2 ± 0.2 |
|               | 40 mg                       | 0.8 ± 0.1             | 1.5 ± 0.2 |
|               | 30 mg                       | 3.0 ± 0.4             | 5.0 ± 0.6 |
|               | 20 mg                       | 6.8 ± 1.1             | 3.9 ± 0.5 |

vigorous shaking) at the same mass to volume ratio (50/40/30/20 mg in 20 ml). In the case of FD BPAC, the subsequent nucleation of CBS occurs inside the bulk liquid phase, in contrast with BPAC, where the nucleation of CBS occurs primarily in the surface layer of coarse BPAC particles (see photo- and video data in the ESI).

Results of DLS experiments, aimed to study the nucleation of CBS in FD BPAC and BPAC systems in 0.1 M and 0.01 M HCl (Figure 3, Table 2) can be summarized as follows:

In FD BPAC and BPAC systems in 0.1 M HCl the increase of the value of hydrodynamic diameter of the CBS particles begins from  $\sim 0.5 \mu\text{m}$  and reaches 1.1–1.8  $\mu\text{m}$  in 20 minutes. Essential differences in hydrodynamic diameter of the CBS particles in FD BPAC ( $D_h=1.1 \mu\text{m}$ ) and BPAC ( $D_h=1.8 \mu\text{m}$ ) systems in 0.1 M HCl are observed only for large loads of 50 mg.

In FD BPAC and BPAC systems in 0.01 M HCl and small loads (sample mass to volume ratio) the values of hydrodynamic diameters of the CBS particles range within 3.0–6.8  $\mu\text{m}$  (FD BPAC) and 3.9–5.0  $\mu\text{m}$  (BPAC). The largest differences for FD BPAC ( $D_h=0.3\text{--}0.8 \mu\text{m}$ ) and BPAC ( $D_h=1.2\text{--}1.5 \mu\text{m}$ ) are observed at large loads (40–50 mg per 20 ml) in 0.01 M HCl.

Smaller sample weights and the decrease in HCl concentration results in the increase in the hydrodynamic diameters of CBS particles of FD BPAC and BPAC systems. Significant variation in the measured value of the hydrodynamic diameter of CBS particles in BPAC in 0.01 M HCl can be explained that in the case of FD BPAC the nucleation of CBS occurs inside the bulk liquid phase, while the vials with BPAC always contained crystalline precipitate (and suspension) of the starting BPAC. In addition, the concentration of HCl solution also affects the composition and phase ratio of the precipitate. As two extreme cases, one can propose two results: 1) CBS; 2) BiOCl. This will be the focus of the future work, as well as comparison of dissolution behavior of FD BPAC with starting BPAC and nucleation of CBS in artificial gastric juice.<sup>[30]</sup> To summarize, the results of this study provide the grounds to choose the concentration of HCl and the ratio of the components yielding a colloid solution with required particle sizes ranging from 0.3 to 7  $\mu\text{m}$ .

#### 4. Conclusion

Process design for freeze-drying the BPAC solution in TBA/water co-solvent system was carried out with use of low-

temperature powder x-ray diffraction and thermal analysis methods. BPAC formed an amorphous freeze concentrate on cooling and remain amorphous during freeze-drying and subsequent storage. At the first stages of dissolution, FD BPAC forms a homogeneous solution; subsequent nucleation of CBS occurs inside the bulk liquid phase, in contrast with BPAC, where the nucleation of CBS occurs primarily in the surface layer of coarse BPAC particles. This study is likely to provide a basis for further development of bismuth-based formulations with enhanced dissolution rate for bismuth-based triple therapy, where FD BPAC simultaneously acts as a carrier and an active ingredient.

#### Funding

This study was supported by the Russian Foundation for Basic Research (project no. 17-03-00784-A).

#### ORCID

Andrey G. Ogienko  <http://orcid.org/0000-0001-9907-7355>

#### References

- [1] Gorbach, S. L. Bismuth Therapy in Gastrointestinal Diseases. *Gastroenterology* **1990**, *99*, 863–875. DOI: [10.1016/0016-5085\(90\)90983-8](https://doi.org/10.1016/0016-5085(90)90983-8).
- [2] Lambert, J. R.; Midolo, P. The Actions of Bismuth in the Treatment of Helicobacter pylori Infection. *Aliment. Pharmacol. Ther.* **1997**, *11*, 27–33. DOI: [10.1046/j.1365-2036.11.s1.13.x](https://doi.org/10.1046/j.1365-2036.11.s1.13.x).
- [3] Williams, D. R. Analytical and Computer Simulation Studies of a Colloidal Bismuth Citrate System Used as an Ulcer Treatment. *J. Inorg. Nucl. Chem.* **1977**, *39*, 711–714. DOI: [10.1016/0022-1902\(77\)80600-3](https://doi.org/10.1016/0022-1902(77)80600-3).
- [4] Briand, G. G.; Burford, N. Bismuth Compounds and Preparations with Biological or Medicinal Relevance. *Chem. Rev.* **1999**, *9*, 2601–2957. DOI: [10.1021/cr980425s](https://doi.org/10.1021/cr980425s).
- [5] Sun, Q.; Liang, X.; Zheng, Q.; Liu, W.; Xiao, S.; Gu, W.; Lu, H. High Efficacy of 14-Day Triple Therapy-Based, Bismuth-Containing Quadruple Therapy for Initial Helicobacter pylori Eradication. *Helicobacter* **2010**, *15*, 233–238. DOI: [10.1111/j.1523-5378.2010.00758.x](https://doi.org/10.1111/j.1523-5378.2010.00758.x).
- [6] Megraud, F. The Challenge of Helicobacter pylori Resistance to Antibiotics: The Comeback of Bismuth-Based Quadruple Therapy. *Therap. Adv. Gastroenterol.* **2012**, *5*, 103–109. DOI: [10.1177/1756283X11432492](https://doi.org/10.1177/1756283X11432492).
- [7] Graham, D. Y.; Lew, G. M.; Malaty, H. M.; Evans, D. G.; Evans, D. J.; Klein, P. D.; Alpert, L. C.; Genta, R. M. Factors Influencing the Eradication of Helicobacter-Pylori with Triple Therapy. *Gastroenterology* **1992**, *102*, 493–496. DOI: [10.1016/0016-5085\(92\)90095-G](https://doi.org/10.1016/0016-5085(92)90095-G).
- [8] Saleem, A.; Qasim, A.; O'Connor, H. J.; O'Morain, C. A. Pylora for the Eradication of Helicobacter pylori Infection. *Expert. Rev. Anti. Infect. Ther.* **2009**, *7*, 793–799. DOI: [10.1586/eri.09.55](https://doi.org/10.1586/eri.09.55).
- [9] Wagstaff, A. J.; Benfield, P.; Monk, J. P. Colloidal Bismuth Subcitrate - a Review of Its Pharmacodynamic and Pharmacokinetic Properties, and Its Therapeutic Use in Peptic-Ulcer Disease. *Drugs* **1988**, *36*, 132–157. DOI: [10.2165/00003495-198836020-00002](https://doi.org/10.2165/00003495-198836020-00002).
- [10] Yukhin, Y. M.; Afonina, L. I.; Lyakhov, N. Z.; Daminov, A. S.; Naydenko, E. S. Method of Producing Bismuth-Potassium Ammonium Citrate. R.F. Patent 2,530 2014, 897, October 20

- [11] Furlan, D.; Felice, S. S. Bismuth-Containing Composition Suitable for Therapeutic Use. U.S. Patent 1990, 4, 965,382, January 18.
- [12] Bos, P. J. H.; Engel, D. J. C.; De, J. H. Bismuth Containing Composition and Method for the Preparation Thereof. U.S. Patent 1989, 4, 801,608, January 31.
- [13] Liu, J. S. Physical Characterization of Pharmaceutical Formulations in Frozen and Freeze-Dried Solid States: techniques and Applications in Freeze-Drying Development. *Pharm. Dev. Technol.* **2006**, *11*, 3–28. DOI: [10.1080/10837450500463729](https://doi.org/10.1080/10837450500463729).
- [14] Kasper, J. C.; Winter, G.; Friess, W. Recent Advances and Further Challenges in Lyophilization. *Eur. J. Pharm. Biopharm.* **2013**, *85*, 162–169. DOI: [10.1016/j.ejpb.2013.05.019](https://doi.org/10.1016/j.ejpb.2013.05.019).
- [15] Wang, W. Lyophilization and Development of Solid Protein Pharmaceuticals. *Int. J. Pharm.* **2000**, *203*, 1–60. DOI: [10.1016/S0378-5173\(00\)00423-3](https://doi.org/10.1016/S0378-5173(00)00423-3).
- [16] Madhally, S. V.; Matthew, H. W. T. Porous Chitosan Scaffolds for Tissue Engineering. *Biomaterials* **1999**, *20*, 1133–1142. DOI: [10.1016/S0142-9612\(99\)00011-3](https://doi.org/10.1016/S0142-9612(99)00011-3).
- [17] Tang, X. C.; Pikal, M. J. Design of Freeze-Drying Processes for Pharmaceuticals: practical Advice. *Pharm. Res.* **2004**, *21*, 191–200. DOI: [10.1023/B:PHAM.0000016234.73023.75](https://doi.org/10.1023/B:PHAM.0000016234.73023.75).
- [18] Vessot, S.; Andrieu, J. A Review on Freeze Drying of Drugs with Tert - Butanol (TBA) + Water Systems: characteristics, Advantages, Drawbacks. *Dry. Technol.* **2012**, *30*, 377–385. DOI: [10.1080/07373937.2011.628133](https://doi.org/10.1080/07373937.2011.628133).
- [19] Teagarden, D. L.; Baker, D. S. Practical Aspects of Lyophilization Using Non-Aqueous co-Solvent Systems. *Eur. J. Pharm. Sci.* **2002**, *15*, 115–133. DOI: [10.1016/S0928-0987\(01\)00221-4](https://doi.org/10.1016/S0928-0987(01)00221-4).
- [20] Daoussi, R.; Vessot, S.; Andrieu, J.; Monnier, O. Sublimation Kinetics and Sublimation End-Point Times during Freeze-Drying of Pharmaceutical Active Principle with Organic co-Solvent Formulations. *Chem. Eng. Res. Des.* **2009**, *87*, 899–907. DOI: [10.1016/j.cherd.2008.09.007](https://doi.org/10.1016/j.cherd.2008.09.007).
- [21] Kasraian, K.; DeLuca, P. P. The Effect of Tertiary Butyl Alcohol on the Resistance of the Dry Product Layer during Primary Drying. *Pharm. Res.* **1995**, *12*, 491–495. DOI: [10.1023/A:1016285425670](https://doi.org/10.1023/A:1016285425670).
- [22] Oesterle, J.; Franks, F.; Auffret, T. The Influence of Tertiary Butyl Alcohol and Volatile Salts on the Sublimation of Ice from Frozen Sucrose Solutions: implications for Freeze-Drying. *Pharm. Dev. Technol.* **1998**, *3*, 175–183. DOI: [10.3109/10837459809028493](https://doi.org/10.3109/10837459809028493).
- [23] Cui, J. X.; Li, C. L.; Deng, Y. J.; Wang, Y. L.; Wang, W. Freeze-Drying of Liposomes Using Tertiary Butyl Alcohol/Water Cosolvent Systems. *Int. J. Pharm.* **2006**, *312*, 131–136. DOI: [10.1016/j.ijpharm.2006.01.004](https://doi.org/10.1016/j.ijpharm.2006.01.004).
- [24] Ogienko, A. G.; Bogdanova, E. G.; Stoporev, A. S.; Ogienko, A. A.; Shinkorenko, M. P.; Yunoshev, A. S.; Manakov, A. Y. Preparation of Fine Powders by Clathrate-Forming Freeze-Drying: A Case Study of Ammonium Nitrate. *Mendeleev Commun.* **2018**, *28*, 211–213. DOI: [10.1016/j.mencom.2018.03.035](https://doi.org/10.1016/j.mencom.2018.03.035).
- [25] Phillies, G. D. J. Quasi-Elastic Light Scattering. *Anal. Chem.* **1990**, *62*, 1049–1057.
- [26] Rosso, J.-C.; Carbonnel, L. Le système eau-butanol tertiaire. *C. R. Acad. Sci. Paris Ser. C.* **1968**, *267*, 4.
- [27] Ott, J. B.; Goates, J. R.; Waite, B. A. (Solid + Liquid) Phase-Equilibria and Solid-Hydrate Formation in Water + Methyl, + Ethyl, + Isopropyl, and + Tertiary Butyl Alcohols. *J. Chem. Thermodyn.* **1979**, *11*, 739–746. DOI: [10.1016/0021-9614\(79\)90005-3](https://doi.org/10.1016/0021-9614(79)90005-3).
- [28] Woznyj, M.; Ludemann, H. D. The Pressure of Dependence of the Phase-Diagram T-Butanol Water. *Z. Naturforsch.* **1985**, *40A*, 693–698. DOI: [10.1515/zna-1985-0707](https://doi.org/10.1515/zna-1985-0707).
- [29] Machida, T. A Study of Intragastric pH in Patients with Peptic Ulcer-with Special Reference to the Clinical Significance of Basal pH Value. *Gastroenterol. Jpn.* **1981**, *16*, 447–458. DOI: [10.1007/BF02774516](https://doi.org/10.1007/BF02774516).
- [30] Chen, L.; Xu, Y.; Fan, T.; Liao, Z.; Wu, P.; Wu, X.; Chen, X. D. Gastric Emptying and Morphology of a ‘near Real’ in Vitro Human Stomach Model (RD-IV-HSM). *J. Food Eng.* **2016**, *183*, 1–8. DOI: [10.1016/j.jfoodeng.2016.02.025](https://doi.org/10.1016/j.jfoodeng.2016.02.025).